PERGAMON

Available online at www.sciencedirect.com
SCIENCE DIRECT®

Engineering Fracture Mechanics 70 (2003) 1659–1674

Engineering Fracture Mechanics

www.elsevier.com/locate/engfracmech

On estimating stress intensity factors and modulus of cohesion for fractal cracks

Michael P. Wnuk [a], Arash Yavari [b,*]

[a] Department of Civil Engineering and Mechanics, University of Wisconsin, Milwaukee, WI 53201, USA
[b] Graduate Aeronautical Laboratories, California Institute of Technology, Pasadena, CA 91125, USA

Received 6 September 2001; received in revised form 18 June 2002; accepted 4 September 2002

Abstract

Existing solutions for the singular stress field in the vicinity of a fractal crack tip have been adapted for a somewhat modified problem. Since the integration along the fractal curve is prohibitive and does not lend itself to the presently available mathematical treatments, a simplified one has replaced the original problem. The latter involves a smooth crack embedded in a singular stress field, for which the order of singularity is adjusted to match exactly the one obtained from the analyses pertaining to the fractal crack. Of course, this is only an approximation, and we may only hope that it leads toward correct results, at least in a cursory sense. The advantage of such an approach becomes obvious when one inspects the final closed-form solutions for (a) the stress intensity factor in mode I fractal fracture, and (b) cohesion modulus, which results from the cohesive zone model and serves as a measure of the material resistance to crack propagation. As expected for the fractal geometry employed here, our results are strongly dependent on the fractal dimension D (or roughness exponent H).

Keywords: Fractal fracture; Fractal crack; Stress intensity factor; Modulus of cohesion

1. Introduction

Experimentally observed patterns of fracture exhibit irregular and fragmented nature at a level of complexity that cannot be described within the confines of the Euclidean geometry. Therefore, in several fields of science and engineering, including fracture mechanics and contact mechanics, fractal geometry has found numerous applications [1–3]. Such generalizations, of course, are associated with the novel rules for the theory capable to represent the structure of stress and strain singularities present at the tip of a fractal crack. A number of basic concepts, such as stress, surface traction, specific surface energy, J-integral, modulus of cohesion and other parameters essential for mathematical depiction of the fracture process had to be redefined [4–16]. It should be mentioned that there have been some studies on size effects using fractal geometry techniques by Carpinteri and his coworkers [17–21]. Despite this concentrated effort, certain

* Corresponding author. Tel.: +1-626-395-2178; fax: +1-626-449-2677.
E-mail address: arash@aero.caltech.edu (A. Yavari).

0013-7944/03/$ - see front matter
doi:10.1016/S0013-7944(02)00205-9

important concepts, which form the foundation of the classical fracture mechanics, are still either undefined or vaguely defined for fractal cracks. This includes the stress intensity factor K_I for a Griffith crack and the cohesion modulus for a Barenblatt crack [16]. The latter measures material resistance to crack propagation, and relates the specific distribution of the cohesive tractions restraining separation of the opposite sides of a growing crack, or a virtually growing crack, to the well-known concept of material *toughness*.

The problem posed here defies an exact solution. When the fractal geometry is taken into account, even the basic concepts of calculus such as line or area integrals must be reconsidered [22,23]. The problem may be solved, though, if one accepts a certain simplifying assumption. This assumption is described in the sequel, and the proposed closed-form solutions are generated. These solutions reflect the infinitely complex nature of fractal objects, such as cracks, that are embedded within the Euclidean space. The fractal dimension, D, usually a noninteger, is a measure of how strongly a given fractal entity diverges from its Euclidean counterpart. As it turns out, this fractal dimension—being a geometrical characteristic of the fracture surface, enters as a new independent variable in most of the pertinent equations of the fractal fracture mechanics. In this paper we estimate mode I stress intensity factor and modulus of cohesion for self-similar and self-affine fractal cracks. As a first approximation a smooth crack is embedded in the stress field of the fractal crack.

This paper is structured as follows: In Section 2, mode I stress intensity factor of a (self-similar or self-affine) fractal crack is estimated using the method of imaginary smooth crack. Section 3 discusses a recently developed fractal cohesive fracture theory [16] and gives an estimate for the fractal cohesion modulus, again using the method of imaginary smooth crack. Conclusions are given in Section 4. The derivation of stress intensity factor for a smooth crack embedded in the stress field of a corresponding fractal crack is given in Appendix A.

2. Stress intensity factor for a fractal crack

A noteworthy phenomenon in the theoretical studies of fractal fracture mechanics is the change of the order of stress singularity at the crack tip. For a fractal version of the Griffith crack the familiar singularity of $r^{-1/2}$ is replaced by a somewhat weaker singularity for the near-tip stress, $r^{-\alpha}$, where α depends on the fractal dimension D, namely

$$\alpha = \frac{2-D}{2}, \quad 1 \leqslant D \leqslant 2 \tag{1a}$$

for a self-similar crack and

$$\alpha = \begin{cases} \dfrac{2H-1}{2H}, & \frac{1}{2} \leqslant H \leqslant 1 \\ 0, & 0 \leqslant H \leqslant \frac{1}{2} \end{cases} \tag{1b}$$

for a self-affine crack (see [15] for more details). Note that D varies from 1 to 2, in which the lower bound corresponds to the case of smooth crack, while the upper limit represents an infinitely irregular fractal curve that "fills the plane", and can be envisioned as a void contained within the plane. For this latter case $\alpha = 0$, and thus the singularity disappears altogether. For the case of a self-affine fractal crack H varies from 0 to 1. However for extremely irregular self-affine cracks for which $0 \leqslant H \leqslant \frac{1}{2}$ there is no stress singularity [15]. Therefore, we consider only $\frac{1}{2} \leqslant H \leqslant 1$. As we proceed to show in what follows, all the important fracture mechanics parameters will reflect the D (or H)-dependence in addition to any other well-established functional relationships. This geometrical "fractal effect" has to be considered separately from mechanical factors such as applied loads, specimen configuration and the crack size, and separately from the material properties that define the cohesion modulus for a smooth crack.

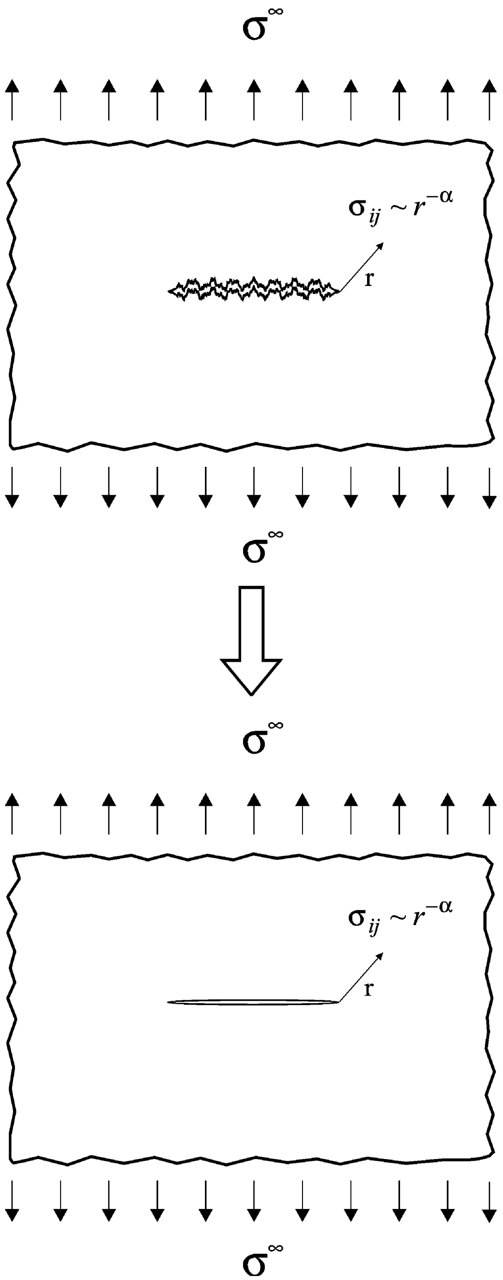

Fig. 1. Method of imaginary smooth crack: (a) a fractal crack in an infinite solid, (b) a smooth crack embedded in the stress field of the fractal crack.

Let us take a closer look at the stress intensity factor, a basic concept in linear elastic fracture mechanics. After a brief discussion of the K-factor for a smooth crack we will extend the definition onto a fractal crack. First, let us invoke the classic integral representation of the stress intensity factor, stemming from the Green's function approach [24]

$$K_{\mathrm{I}} = 2\sqrt{\frac{a}{\pi}} \int_0^a \frac{p(x)\,\mathrm{d}x}{\sqrt{a^2 - x^2}} \tag{2}$$

This formula is valid for an arbitrary even distribution of pressure $p(x)$ exerted over the surfaces of the pressurized 2D crack of half-length 'a', and it corresponds to the following mixed boundary value problem defined along the edge $y = 0$ of the semi-infinite plane

$$\begin{cases} p(x) = \sigma & \text{for } |x| < a \\ u_y(x) = 0 & \text{for } |x| > a \end{cases} \tag{3}$$

When the pressurized crack problem is solved, then a superposition of the remotely applied tension $p(x) = -\sigma$ removes the stress from the crack rendering it stress-free as anticipated. It is noted that for a constant $p(x) = \sigma$, formula (2) readily reduces to $K_{\mathrm{I}} = \sigma\sqrt{\pi a}$.

Generalization of the formula (2) for a fractal crack with dimension D (or Hurst exponent H) is not a well-defined problem (see [15,16]). This is why all the existing results to date are based on dimensional analysis considerations. Here we try to go one step forward. Our basic assumption is that when the correct order of stress singularity, $r^{-\alpha}$ is applied to a smooth crack in lieu of the Griffith $r^{-1/2}$ result, in other words—when the fractal crack is replaced by a smooth crack embedded in the fractal singular stress field, then proceeding with the problem one arrives at a first approximation to the exact (and unknown) solutions (see Fig. 1). The objective of this simplification is to reduce the case of integration on fractal curve in the plane to that of common calculus. Generalization of the formula (2) for a stress field of the type $r^{-\alpha}$ leads to the following expression:

$$K_{\mathrm{I}}^{\mathrm{f}} = \frac{a^{\alpha-1}}{\pi^{2\alpha-\frac{1}{2}}} \int_0^a \frac{(a+x)^{2\alpha} + (a-x)^{2\alpha}}{(a^2-x^2)^{\alpha}} p(x)\,\mathrm{d}x \tag{4a}$$

where '$2a$' is the "nominal" crack length defined as

$$2a = \sup_{\ell \subset \mathbb{R}^2} \|P_\ell(\mathscr{F})\| \tag{4b}$$

where $\mathscr{F}$ is the boundary of the fractal crack, P_ℓ is the projection operator on a lime ℓ in the plane of the fractal crack and $\|\cdot\|$ is the standard norm in $\mathbb{R}^2$. Eq. (4a) is derived in Appendix A. Choosing symbol s for a nondimensional coordinate, $s = x/a$, and letting $p(x)$ to be equal to σ, a constant remotely applied stress, we reduce expression (4a) and (4b) as follows:

$$K_{\mathrm{I}}^{\mathrm{f}} = \frac{\sigma a^{\alpha}}{\pi^{2\alpha-\frac{1}{2}}} \int_0^1 \frac{(1+s)^{2\alpha} + (1-s)^{2\alpha}\,\mathrm{d}s}{(1-s^2)^{\alpha}} \tag{5}$$

or, in terms of D, for a self-similar crack

$$K_{\mathrm{I}}^{\mathrm{f}} = \frac{\sigma\sqrt{\pi a^{2-D}}}{\pi^{2-D}} \int_0^1 \frac{(1+s)^{2-D} + (1-s)^{2-D}}{(1-s^2)^{(2-D)/2}}\,\mathrm{d}s \tag{6}$$

For a self-affine crack, we use Eq. (1b) to obtain

$$K_{\mathrm{I}}^{\mathrm{f}} = \frac{\sigma\sqrt{\pi a^{(2H-1)/H}}}{\pi^{(2H-1)/H}} \int_0^1 \frac{(1+s)^{(2H-1)/H} + (1-s)^{(2H-1)/H}}{(1-s^2)^{(2H-1)/2H}}\,\mathrm{d}s \tag{7}$$

When these expressions are compared with the $K_{\mathrm{I}}^{\mathrm{f}}$ predicted on the basis of the dimensional analysis [15]

$$K_{\mathrm{I}}^{\mathrm{f}} = \chi(D)\sigma\sqrt{\pi a^{2-D}} \tag{8a}$$

$$K_{\mathrm{I}}^{\mathrm{f}} = \psi(H)\sigma\sqrt{\pi a^{(2H-1)/H}} \tag{8b}$$

then one arrives at the following closed-form definition of the χ and ψ functions. The comparison yields

$$\chi(D) = \frac{1}{\pi^{2-D}} \int_0^1 \frac{(1+s)^{2-D} + (1-s)^{2-D}}{(1-s^2)^{(2-D)/2}} \, \mathrm{d}s \tag{9}$$

$$\psi(H) = \frac{1}{\pi^{(2H-1)/H}} \int_0^1 \frac{(1+s)^{(2H-1)/H} + (1-s)^{(2H-1)/H}}{(1-s^2)^{(2H-1)/2H}} \, \mathrm{d}s \tag{10}$$

These integrals can be easily evaluated numerically. Figs. 2a and b show the result of the numerical calculations of the functions χ and ψ.

For a self-similar fractal crack, $\chi(D)$ increases from 1, at $D = 1$, yielding the classical fracture mechanics result, $K_\mathrm{I} = \sigma\sqrt{\pi a}$, to a value of 2, yielding $K_\mathrm{I} = 2\sigma\sqrt{\pi}$ for D approaching 2 (see Fig. 2a). The latter limit corresponds to a plane filling fractal crack. This limit can be thought of being equivalent to an elliptic hole. Note that for a hole in an infinite medium stress intensity factor may be likened to a stress concentration

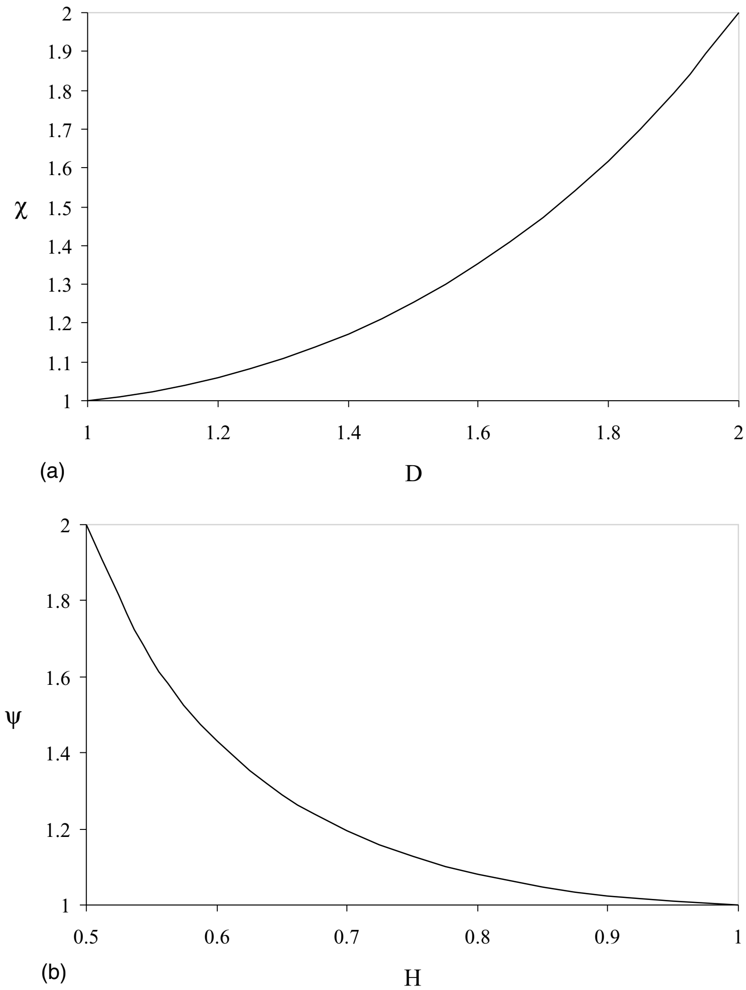

Fig. 2. (a) Variation of χ with D, (b) variation of ψ with H.

factor, which should be equal to $1 + 2(a/b)$, where $2a$ and $2b$ are the principal diameters of the ellipse. It is seen that our approximation suggesting a factor of $2\sqrt{\pi}$ corresponds to $a/b = \sqrt{\pi} - (1/2)$. It is expected that our approximation is more accurate for smaller D because the smaller the fractal dimension, the less irregular the fractal crack. It is noted that the function $\chi(D)$ increases with D, implying a greater effort needed to bring the external loads to its critical level, which coincides with the onset of crack propagation. Any direct comparison, however, is unfortunately not possible here. This is due to a different dimension of the K-factor, which changes continuously with the fractal dimension D as it varies within the interval $D \in (1, 2)$ (direct comparison of quantities of different dimension is not physically meaningful).

For a self-affine fractal crack, the function ψ is a decreasing function of H. The variation of this function with H is shown in Fig. 2b. The limit $H = 0.5$ corresponds to a hole (similar to $D = 2$). As H increases, ψ decreases until it reaches unity for $H = 1$. We expect to have the largest error for $H = 0.5$.

In the present approximation, the geometry of the fractal crack is replaced by a corresponding imaginary smooth crack with length equal to the nominal length of the fractal crack. However, the stress field changes with D (or H) as the fractal dimension (roughness exponent) of the crack changes. The solutions obtained using the imaginary smooth crack method are exact for $D = 1$ (or $H = 1$). We know that as D increases (H decreases) the fractal crack becomes more and more irregular and consequently approximating it with a smooth crack becomes less and less accurate.

3. Barenblatt fractal crack and the associated cohesion modulus

Recently Yavari [16] generalized Barenblatt's cohesive fracture theory for fractal cracks. He showed the equivalence of fractal Griffith and Barenblatt theories. Despite entirely different modeling concepts employed by Griffith [25,26], who used the global formulation, and by Barenblatt [27] who employed a local approach, both models of the fracture process are mathematically equivalent (see [28,29]). Therefore, it is reasonable to assume that for a fractal crack represented by a cohesive zone model, the same stress singularity applies, namely $r^{-\alpha}$ [16]. For the boundary conditions of the type (3), but modified for an extended crack, we have

$$p(x) = \begin{cases} \sigma, & 0 < x < c \\ \sigma - S, & c < x < a \end{cases} \tag{11}$$

Here, 'a' denotes the half-length of the extended crack, 'c' is the half-length of the physical crack, while S denotes the cohesive stress defined over the interval $c < x < a$. In the context of the cohesive zone model, no infinite stresses are allowed to exist at the crack tip. This implies that the total K-factor resulting from a superposition of stress fields due to applied stress σ, and to the cohesive stress, S, must vanish. Using this statement, and combining the definition (2) with the boundary conditions (11), we obtain

$$2\sqrt{\frac{a}{\pi}}\left[\int_0^c \frac{\sigma\,\mathrm{d}x}{\sqrt{a^2 - x^2}} + \int_c^a \frac{\sigma - S\,\mathrm{d}x}{\sqrt{a^2 - x^2}}\right] = 2\sqrt{\frac{a}{\pi}}\left[\int_0^a \frac{\sigma\,\mathrm{d}x}{\sqrt{a^2 - x^2}} - \int_c^a \frac{S\,\mathrm{d}x}{\sqrt{a^2 - x^2}}\right] = 0 \tag{12}$$

This is the so-called finiteness condition written out for a smooth crack, compare Wnuk [30]. The first integral in Eq. (12) is elementary and reduces to $\sigma\pi/2$. Thus we have

$$\frac{\pi\sigma}{2} = \int_c^a \frac{S\,\mathrm{d}x}{\sqrt{a^2 - x^2}} \tag{13}$$

If the cohesive traction S is expressed as a function of the reference stress S_0, material properties ω and n, and the coordinate x, i.e.,

$$S = S_0 \widetilde{G}(x, \omega, n) \tag{14}$$

Then Eq. (14) can be cast into the form [31]

$$Q = \int_c^a \frac{\widetilde{G}(x,\omega,n)\,\mathrm{d}x}{\sqrt{a^2-x^2}} = \int_m^1 \frac{G(s,\omega,n)\,\mathrm{d}s}{\sqrt{1-s^2}}, \quad Q = \frac{\pi\sigma}{2S_0}, \quad m = \frac{c}{a} \tag{15}$$

An equivalent form of this expression involves the modulus of cohesion K_{coh}, rather than the loading parameter Q. Multiplying Q by the factor $(2/\pi)S_0(\pi a)^{1/2}$ we convert the loading factor into the cohesion modulus [1], namely

$$K_{\mathrm{coh}} = \frac{2}{\pi} S_0 \sqrt{\pi a} \int_m^1 \frac{G(s)\,\mathrm{d}s}{\sqrt{1-s^2}} \tag{16}$$

For compactness we have used here the symbol $G(s)$ instead of $G(s,\omega,n)$. For further discussion it is beneficial to replace the variable s by the nondimensional distance measured from the crack tip, $\lambda = x_1/R$, where $R = a - c$. Using the simple relation between the two variables

$$\lambda = \frac{x_1}{R} = \frac{x-c}{a-c} = \frac{s-m}{1-m} \tag{17}$$

we obtain

$$s = (1-m)\lambda + m \tag{18}$$

With this substitution the denominator in the integral of (16) can be written as

$$\sqrt{1-s^2} = [(1-s)(1+s)]^{1/2} = \{[1-m-(1-m)\lambda][1+m+(1-m)\lambda]\}^{1/2} \tag{19}$$

Now, we shall restrict the considerations to the small scale yielding range, for which $R \ll c$ and $m \to 1$. These assumptions reduce the expression (19) to $\sqrt{2(1-m)(1-\lambda)}$, and the formula (16) assumes then the form

$$K_{\mathrm{coh}} = \frac{2}{\pi} S_0 \sqrt{\pi a} \int_0^1 \frac{G(\lambda)(1-m)\,\mathrm{d}\lambda}{\sqrt{2(1-m)(1-\lambda)}} = \frac{\sqrt{2(1-m)}}{\pi} S_0 \sqrt{\pi a} \int_0^1 \frac{G(\lambda)\,\mathrm{d}\lambda}{\sqrt{1-\lambda}} \tag{20}$$

Since within the small scale yielding range $(1-m)$ can be replaced by the ratio R/c and 'c' can be substituted for 'a', we have [2]

$$K_{\mathrm{coh}} = S_0 \sqrt{\frac{2R}{\pi}} \int_0^1 \frac{G(\lambda)\,\mathrm{d}\lambda}{\sqrt{1-\lambda}} \tag{21}$$

This result is valid for a smooth crack. Various forms of the cohesive stress distributions $G(\lambda)$ were considered by Wnuk et al. [32] and Wnuk and Legat [31]. One such form involves a power function and an exponential, namely

$$G(\lambda,\omega,n) = \lambda^n \exp[\omega(1-\lambda)], \quad 0 \leqslant \lambda \leqslant 1 \tag{22}$$

Here, n and ω are so-called microstructural constants. Function G rises steeply from zero at the crack tip ($\lambda = 0$), reaches a maximum at the outer edge of the process zone at $\lambda_{\max} = n/\omega$, and then gradually falls off

[1] It should be noted that this definition of the cohesive modulus differs from that of Barenblatt by a constant factor. Advantage of the present notation is that our K_{coh} may be directly identified with the material fracture toughness, K_{C} or K_{IC}.

[2] Frequently this equation is inverted to provide an estimate of the characteristic material length

$$R_c = \frac{\pi}{2W^2}\left(\frac{K_{\mathrm{IC}}}{S_0}\right)^2$$

where W denotes the integral appearing in Eq. (2) and the cohesion modulus K_{coh} has been replaced by the material toughness, K_{IC}.

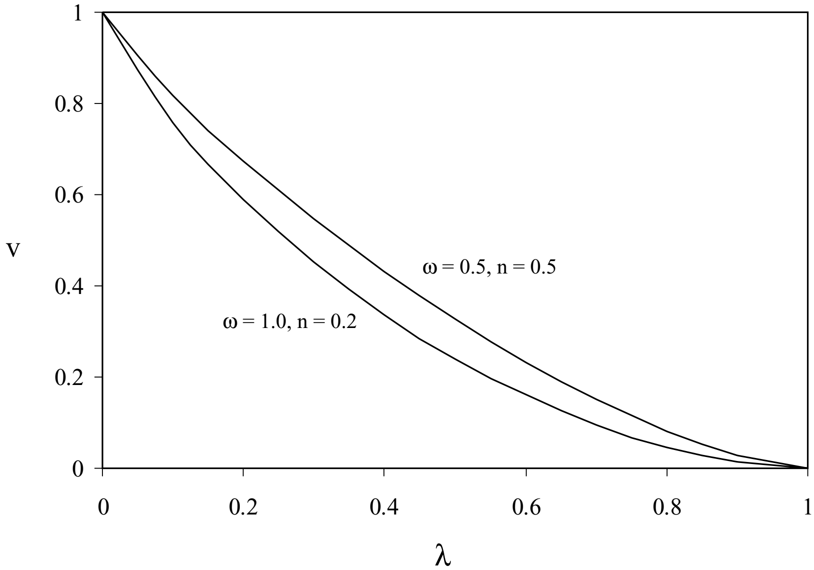

Fig. 3. The profiles of the extended crack shown within the nonlinear end zone for two choices of the material parameters.

to the reference stress $S = S_0$, or $G = 1$ at the end of the nonlinear zone, $x_1 = R$ (or $\lambda = 1$). This behavior is illustrated in Fig. 3 for $\omega = 1$, $n = 0.2$, and $\omega = 0.5$, $n = 0.5$.

A more meaningful and physically significant representation of the G-distribution is provided by plotting G vs. the opening displacement, v. Such a graph establishes a "law of separation", which is built into every cohesive zone model of a crack. It is noteworthy that this representation of the separation law expressing the cohesion closure traction as a function of the relative displacement between the crack faces at a certain fixed point, is applicable equally well to smooth and fractal cracks.

Conversion of the relation G vs. λ, as given by Eq. (22), into the separation law G vs. v, can be accomplished by using the interpolation formula proposed by Wnuk and Legat [31]. According to this formula the opening displacement in mode I crack can be obtained from two known functions that within the small scale yielding range represent exactly the crack profile within the nonlinear zone, namely

$$\begin{aligned} \Lambda_0(\lambda) &= \sqrt{1-\lambda} - \frac{\lambda}{2}\ln\left[\frac{1+\sqrt{1-\lambda}}{1-\sqrt{1-\lambda}}\right], \quad n = 0,\ \ \omega = 0 \\ \Lambda_1(\lambda) &= \sqrt{1-\lambda}\left(1-\frac{1}{2}\lambda\right) - \frac{\lambda^2}{4}\ln\left[\frac{1+\sqrt{1-\lambda}}{1-\sqrt{1-\lambda}}\right], \quad n = 1,\ \ \omega = 0 \end{aligned} \tag{23}$$

For an arbitrary choice of ω and n, both contained within the interval $(0,1)$, the following approximation has been suggested [31]:

$$v(\lambda,\omega,n) = \frac{n+\omega}{\omega+1}\Lambda_1^{\omega+n}(\lambda) - \frac{n-1}{\omega+1}\Lambda_0^{\omega+1}(\lambda) \tag{24}$$

Two curves resulting from this equation for the sets ($\omega = 0.5$, $n = 0.5$) and ($\omega = 1$, $n = 0.2$) are shown in Fig. 4. When the second profile, valid for $\omega = 1$ and $n = 0.2$, is used in conjunction with Eq. (22) subject to the same choice of the parameters ω and n, the variable λ can be eliminated from the formula (22). This leads to a G vs. v relation, since λ has been replaced by the new independent variable v. Operation like this

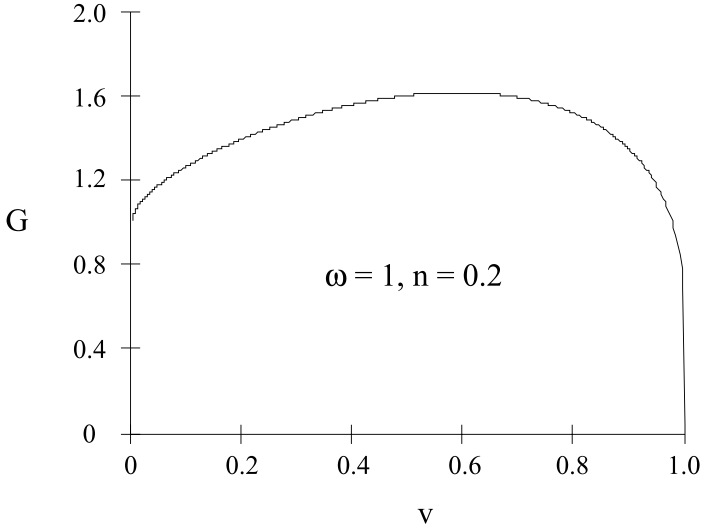

Fig. 4. The separation law shown as nondimensional cohesion force G measured at a certain fixed point versus the normalized crack opening displacement, v.

results in the separation law, G vs. v, as shown in Fig. 4. This figure illustrates the "separation history" at a certain fixed control point, where both S and v are observed. The history begins at an instant when the edge of the extended crack reaches the control point. At this instant the observer placed at the control point will see zero displacement v, while the stress S equals then the reference stress S_0. During the course of the deformation process that proceeds up to the point of fracture, when v reaches the critical value at the end of the graph ($v = 1$), the cohesive stress attains maximum and then drops off to zero as shown in Fig. 4.

These results are directly applicable to the analysis of a fractal crack modeled by the use of the cohesive zone concepts. Now consider a fractal Barenblatt crack [16]. Similar to what was done in Section 2, the method of imaginary smooth crack is utilized, i.e., the fractal crack is replaced by a smooth one without disturbing the stress field (see Fig. 5). Using this approximation for the fractal crack, expression (20) is rewritten as follows:

$$K^{\mathrm{f}}_{\mathrm{coh}} = \frac{2}{\pi} S_0 (\pi a)^{1-\alpha} \int_0^1 \frac{(1-m)^{1-\alpha}}{2^\alpha} \frac{G(\lambda)\,\mathrm{d}\lambda}{(1-\lambda)^\alpha} \tag{25}$$

Note that S_0, ω and n are material properties and independent of D (or H). However, R is in general a function of D (or H). Here we assume that R is independent of D (or H). It should be noted that this is not a separate assumption. We replaced the fractal crack by a smooth crack with the same (nominal) length and end-zone (nominal) length (see Fig. 5). So, R is independent of D (or H) in this approximation. Denoting the integral in (21) by $W = W(\alpha, \omega, n)$, we may simplify the above expression to the form

$$K^{\mathrm{f}}_{\mathrm{coh}} = S_0 \pi^{-\alpha} (2R)^{1-\alpha} W(\alpha, \omega, n) \tag{26}$$

Now, when we test the limit of smooth crack, $D = 1$, the expression (26) reduces to

$$K_{\mathrm{coh}} = S_0 \sqrt{\frac{2R}{\pi}} W\left(\frac{1}{2}, \omega, n\right) \tag{27}$$

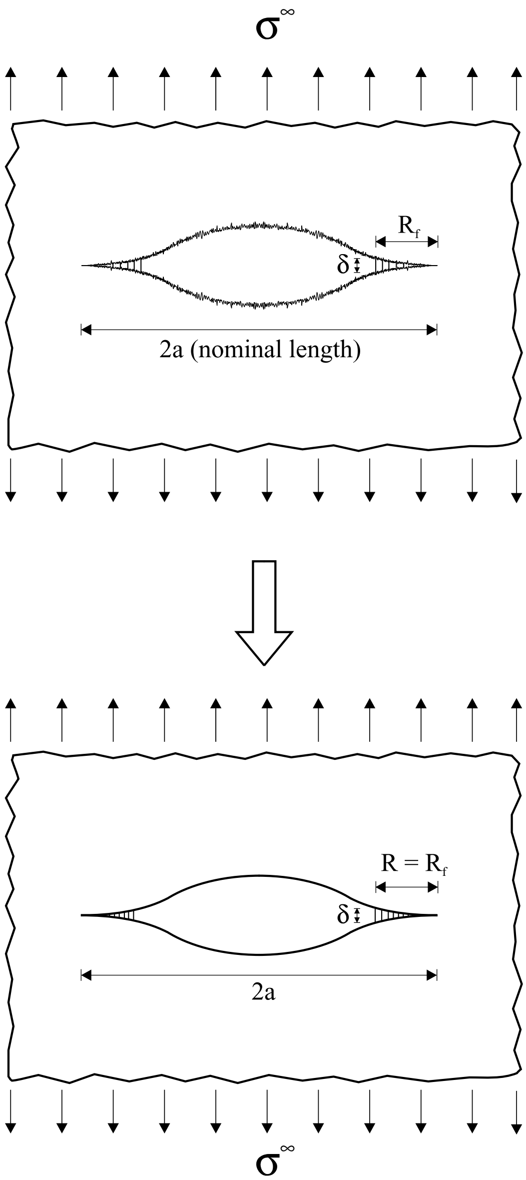

Fig. 5. Method of imaginary smooth crack: (a) a fractal Barenblatt crack in an infinite solid, (b) a smooth Barenblatt crack embedded in the stress field of the fractal crack.

Combining the last two expressions, we may write the final formula for modulus of cohesion as follows:

$$K^{\mathrm{f}}_{\mathrm{coh}} = \Phi(R, D) K_{\mathrm{coh}} \tag{28}$$

Here, the auxiliary function $\Phi(R, D)$ is defined by

$$\Phi(R, D) = (2\pi R)^{(D-1)/2} \eta(\lambda, \omega, n) \tag{29}$$

where

$$\eta(D,\omega,n) = \frac{\displaystyle\int_0^1 \frac{G(\lambda,\omega,n)}{(1-\lambda)^{\alpha(D)}}\,\mathrm{d}\lambda}{\displaystyle\int_0^1 \frac{G(\lambda,\omega,n)}{\sqrt{1-\lambda}}\,\mathrm{d}\lambda} \tag{30}$$

The graphs of the function $\Phi(R,D)$ for R assumed to be certain ratios of the crack length 'a', such as $\rho = R/a = 0.05, 0.1, 0.2, 0.4$ are shown in Fig. 6. To nondimensionalize the function $\Phi(R,D)$ a normalizing constant $a^{(D-1)/2}$ is used, and this yields

$$\phi(D) = \frac{\Phi(R,D)}{a^{(D-1)/2}} = (2\pi\rho)^{(D-1)/2}\eta(D,\omega,n) \tag{31}$$

For $\omega = 1$ and $n = 0.2$ the parameter η varies from 1 to 0.545. These results are valid for a self-similar crack. For a self-affine crack, when $\alpha = \alpha(H)$ is defined by Eq. (1b), a similar representation results for the cohesion modulus of a fractal crack

$$K_{\mathrm{coh}}^{\mathrm{f}} = \Omega(R,H)K_{\mathrm{coh}} \tag{32}$$

Again, the function Ω depends on the length of the cohesive zone R and on the roughness exponent H, namely

$$\Omega(R,H) = (2\pi R)^{(1-H)/2H}\eta_H(H,\omega,n) \tag{33}$$

Note that the function η_H is obtained from η defined by Eq. (30) by substituting $\alpha = \alpha(H)$ for $\alpha = \alpha(D)$, see Eq. (1a) and (1b). When the ratio $\rho = R/a$ is introduced, and a normalizing constant is used, we obtain a nondimensional entity

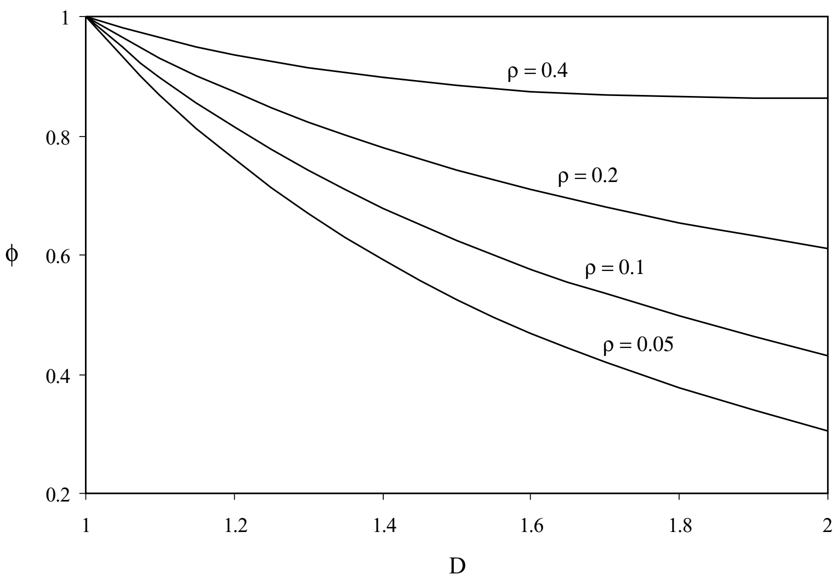

Fig. 6. Auxiliary function $\phi(\rho,D)$, which relates the cohesion modulus of a self-similar fractal crack to that of the corresponding imaginary smooth crack. For various R/a ratios the dependence of ϕ on the fractal dimension D is depicted. It is seen that the largest discrepancy from the classic limit of $\phi = 1$ occurs for the fractal dimension D approaching 2.

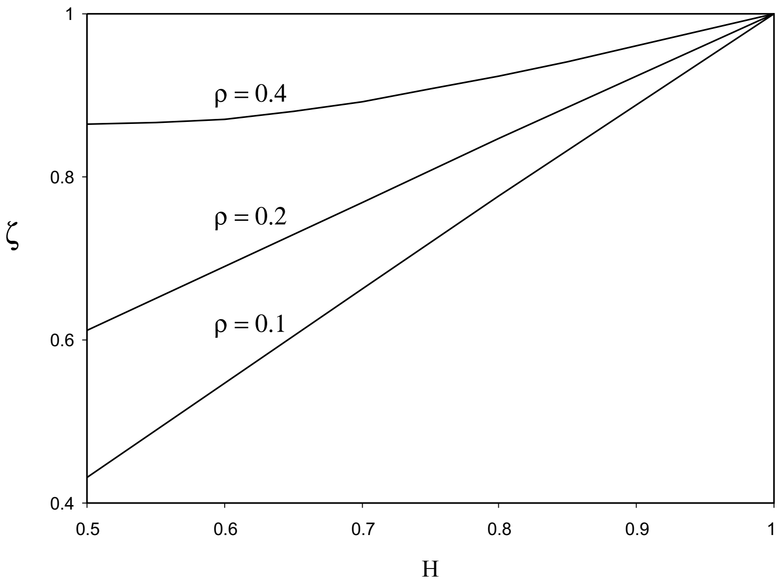

Fig. 7. Auxiliary parameter $\zeta(\rho, H)$ relating the cohesion modulus of a self-affine fractal crack to that of the corresponding imaginary smooth crack, shown as a function of the roughness exponent H, and the R/a ratio. The greatest discrepancy from the classic limit of $\zeta = 1$ occurs at H approaching 0.5.

$$\zeta(H) = \frac{\Omega(R, H)}{a^{(1-H)/2H}} = (2\pi\rho)^{(1-H)/2H}\eta_H(H, \omega, n) \tag{34}$$

This function is plotted against H for several chosen ratios ρ, and fixed material parameters ω and n. The results are shown in Fig. 7. It is seen that as D (or H) changes the dimension of the fractal modulus of cohesion changes. Hence, unfortunately, not much can be concluded from the graphical illustrations of these figures because comparison of quantities with different quantities is meaningless.

4. Conclusions

In this paper we estimate the mode I stress intensity factor for self-similar and self-affine cracks. We also address the issue of the cohesion modulus resulting from the cohesive zone model redefined for the fractal crack of either self-similar or self-affine nature. All results discussed in this work are obtained using the method of imaginary smooth crack. In this method the original problem involving a fractal crack has been replaced by that of a smooth crack embedded in the asymptotic near-tip stress field, which matches exactly the field obtained for a fractal crack.

Our final data pertinent to the fractal cracks exhibit a strong dependence on the fractal dimension D, for a self-similar crack, and on the roughness exponent, H, for a self-affine crack. Two limits of the fractal geometry are discussed in detail. For a self-similar fractal crack the limit of $D = 1$ corresponds to the classic case of a smooth crack, while for D approaching 2 the fractal crack-like object degenerates into a void contained in the plane. Our approximation reduces to the exact result for $D = 1$, while for $D = 2$ the stress intensity factor appears to emulate Neuber's stress concentration coefficient. Graphical illustrations of these new phenomena are provided in Figs. 2, 6 and 7.

Acknowledgements

We are indebted to Prof. G. Ravichandran for a helpful discussion.

Appendix A

Here we intend to show that the near-tip stress field for a fractal crack $\sigma \propto r^{-\alpha}$ can be generated by a suitably chosen Westergaard complex stress potential. Using the "microscope principle" to focus on the immediate vicinity of the crack tip, we consider the potential function Z which depends on $z = x + \mathrm{i}y$ and the fractal crack parameter, α, namely

$$Z(z;\alpha) = \frac{K_{\mathrm{I}}^{\mathrm{f}}}{(2\pi z)^{\alpha}} \tag{A.1}$$

The symbol $K_{\mathrm{I}}^{\mathrm{f}}$ denotes the stress intensity factor for a fractal crack, $K_{\mathrm{I}}^{\mathrm{f}} = K_{\mathrm{I}}^{\mathrm{f}}(\alpha, \sigma, a)$. If the complex variable z is replaced by $r\mathrm{e}^{\mathrm{i}\theta}$, where r and θ are the polar coordinates anchored at the crack tip, then Eq. (A.1) can be rewritten as

$$Z(z;\alpha) = \frac{K_{\mathrm{I}}^{\mathrm{f}}}{(2\pi r)^{\alpha}}[\cos(\alpha\theta) - \mathrm{i}\sin(\alpha\theta)] \tag{A.2}$$

To calculate the components of the stress field, we will need the derivative

$$Z' = \frac{\mathrm{d}Z}{\mathrm{d}z} = \frac{-\alpha K_{\mathrm{I}}^{\mathrm{f}}}{(2\pi)^{\alpha}} z^{-(\alpha+1)} = \frac{-\alpha K_{\mathrm{I}}^{\mathrm{f}}}{(2\pi)^{\alpha}} \frac{1}{r}\{\cos[(\alpha+1)\theta] - \mathrm{i}\sin[(\alpha+1)\theta]\} \tag{A.3}$$

From Eqs. (A.2) and (A.3) we readily obtain

$$\mathrm{Re}\,Z = \frac{K_{\mathrm{I}}^{\mathrm{f}}}{(2\pi)^{\alpha}}\cos(\alpha\theta), \quad \mathrm{Re}\,Z' = -\frac{\alpha}{r}\frac{K_{\mathrm{I}}^{\mathrm{f}}}{(2\pi)^{\alpha}}\cos[(\alpha+1)\theta], \quad \mathrm{Im}\,Z' = \frac{1}{r}\frac{K_{\mathrm{I}}^{\mathrm{f}}}{(2\pi)^{\alpha}}\sin[(\alpha+1)\theta] \tag{A.4}$$

When these expressions are substituted into well-known equations [33]

$$\begin{aligned} \sigma_{xx} &= \mathrm{Re}\,Z - y\,\mathrm{Im}\,Z' \\ \sigma_{yy} &= \mathrm{Re}\,Z + y\,\mathrm{Im}\,Z' \\ \sigma_{xy} &= -y\,\mathrm{Re}\,Z' \end{aligned} \tag{A.5}$$

the following near-tip field for a fractal crack is obtained:

$$\begin{aligned} \sigma_{xx}(r,\theta;\alpha) &= \frac{K_{\mathrm{I}}^{\mathrm{f}}}{(2\pi r)^{\alpha}}\{\cos(\alpha\theta) - \alpha\sin\theta\sin[(\alpha+1)\theta]\} \\ \sigma_{yy}(r,\theta;\alpha) &= \frac{K_{\mathrm{I}}^{\mathrm{f}}}{(2\pi r)^{\alpha}}\{\cos(\alpha\theta) + \alpha\sin\theta\sin[(\alpha+1)\theta]\} \\ \sigma_{xy}(r,\theta;\alpha) &= \frac{K_{\mathrm{I}}^{\mathrm{f}}}{(2\pi r)^{\alpha}}\alpha\sin\theta\cos[(\alpha+1)\theta] \end{aligned} \tag{A.6}$$

This field has a familiar form of an elastic singular stress distribution in the vicinity of the crack tip subject to mode I loading

$$\sigma_{ij}(r,\theta;\alpha) \sim \frac{K_{\mathrm{I}}^{\mathrm{f}}}{(2\pi r)^{\alpha}} f_{ij}(\theta;\alpha) \quad \text{as } r \to 0 \tag{A.7}$$

It is readily seen that for the fractal dimension $D = 1$, when $\alpha = 1/2$, i.e., for the limiting case of a straight crack, Eq. (A.6) reduce to the classic linear fracture mechanics expressions. For the other limiting case of $D = 2$ and $\alpha = 0$, the stress field (A.6) reduces to a nonsingular state of stress, i.e.

$$\sigma_{ij} = O(1) \tag{A.8}$$

This would imply that, when the fractal dimension approaches 2, the fractal crack resembles a 2D void, for which the stress intensity factor $K_{\mathrm{I}}^{\mathrm{f}}$ assumes the meaning of Neuber's stress magnification factor. This point is discussed in a more details in Section 2.

Extending further the concept of the Westergaard potential for a smooth crack embedded in the stress field generated by a fractal crack, and characterized by the fractal singularity exponent α, one obtains

$$Z(z;\alpha) = \int_{-a}^{a} \frac{p(x)[a^2 - x^2]^{\alpha}\,\mathrm{d}x}{\pi(z-x)[z^2 - a^2]^{\alpha}} \tag{A.9}$$

Here $p(x)$ denotes the pressure applied directly to the crack surface. When this expression is substituted into the formula, which defines the K-factor

$$K_{\mathrm{I}}^{\mathrm{f}} = \lim_{x\to a}[2\pi(x-a)]^{\alpha}\,\mathrm{Re}\,Z \tag{A.10}$$

we obtain

$$\widehat{K}_{\mathrm{I}}^{\mathrm{f}} = \frac{1}{(\pi a)^{\alpha}} \int_{-a}^{a} p(x)\left[\frac{a+x}{a-x}\right]^{\alpha} \mathrm{d}x \tag{A.11}$$

The "hat" has been added to emphasize the fact that this expression was derived as an approximation based on the validity of the assumption of "smooth crack embedded in the stress field $r^{-\alpha}$ due to a fractal crack".

Assuming an even distribution of tractions $p(x)$, i.e., $p(-x) = p(x)$, we proceed to evaluate the integral in Eq. (A.11) as follows:

$$\widehat{K}_{\mathrm{I}}^{\mathrm{f}} = \frac{1}{(\pi a)^{\alpha}} \left\{ \int_{a}^{0} p(-x')\left[\frac{a-x'}{a+x'}\right]^{\alpha}(-\mathrm{d}x') + \int_{0}^{a} p(x)\left[\frac{a+x}{a-x}\right]^{\alpha} \mathrm{d}x \right\} \tag{A.12}$$

Note that the dummy variable $x' = -x$ can be renamed as "x" and then both integrals add up, namely

$$\widehat{K}_{\mathrm{I}}^{\mathrm{f}} = \frac{1}{(\pi a)^{\alpha}} \int_{0}^{a} p(x)\left\{\left[\frac{a-x}{a+x}\right]^{\alpha} + \left[\frac{a+x}{a-x}\right]^{\alpha}\right\} \mathrm{d}x \tag{A.13}$$

This leads to

$$\widehat{K}_{\mathrm{I}}^{\mathrm{f}} = \frac{1}{(\pi a)^{\alpha}} \int_{0}^{a} p(x)\frac{(a-x)^{2\alpha} + (a+x)^{2\alpha}}{(a^2 - x^2)^{\alpha}}\,\mathrm{d}x \tag{A.14}$$

This expression represents the K-factor for a true fractal crack within an accuracy of a certain multiplicative constant, say $C = C(\alpha, a)$. Thus, the stress intensity factor that we are seeking reads

$$K_{\mathrm{I}}^{\mathrm{f}} = \frac{C(\alpha,a)}{(\pi a)^{\alpha}} \int_{0}^{a} p(x)\frac{(a-x)^{2\alpha} + (a+x)^{2\alpha}}{(a^2 - x^2)^{\alpha}}\,\mathrm{d}x \tag{A.15}$$

For a truly fractal crack we expect $K_{\mathrm{I}}^{\mathrm{f}}$ to be of the form, cf. Eq. (8a) in Section 2,

$$K_{\mathrm{I}}^{\mathrm{f}} = \chi(\alpha)\sigma\sqrt{\pi a^{2\alpha}} \tag{A.16}$$

in which $\chi(1/2)$ equals one, while pressure p is identified with the remotely applied uniform stress σ. Applying the technique of Hermite boundary interpolation within the interval $\alpha \in (0, 1/2)$, we obtain the matching factor

$$C(\alpha, a) = \left(\frac{a}{\sqrt{\pi}}\right)^{2\alpha-1} \tag{A.17}$$

It is noteworthy that for the classic case of a straight crack, $C(0.5, a) = 1$, while for $\alpha = 0$, $C(0, a) = \sqrt{\pi/a}$. Combining (A.17) with Eq. (A.15), one arrives at the "best approximation" expression for the stress intensity factor associated with a fractal crack under mode I fracture condition, namely

$$K_{\mathrm{I}}^{\mathrm{f}} = \frac{a^{\alpha-1}}{\pi^{2\alpha-1/2}} \int_0^a p(x) \frac{(a-x)^{2\alpha} + (a+x)^{2\alpha}}{(a^2 - x^2)^{\alpha}} \, \mathrm{d}x \tag{A.18}$$

This is identical to the formula (4a) used in the discussions in Section 2. As can be readily verified, the integral in (A.18) reduces to $\pi a p$ when α approaches $1/2$. When this is multiplied by the coefficient standing in front of the integral, $1/\sqrt{\pi a}$, the classic result of $K_{\mathrm{I}} = p\sqrt{\pi a}$ is recovered. Now, for the other extreme case, when D approaches 2, and α becomes zero, the integral yields ($2pa$), while the coefficient in front of it is $\sqrt{\pi}/a$, yielding the stress intensity factor $K_{\mathrm{I}}^{\mathrm{f}} = 2\pi p$. The physical implications of this result, valid for a crack that degenerates to a two-dimensional void, are discussed in Section 2.

References

[1] Mandelbrot BB, Passoja DE, Paullay AJ. Fractal character of fracture surfaces in metals. Nature 1984;308:721–2.
[2] Saouma VE, Barton CC, Gamaledin NA. Fractal characterization of fracture surface in concrete. Engng Fract Mech 1990;35:47–53.
[3] Saouma VE, Barton CC. Fractals, fractures, and size effect in concrete. J Engng Mech 1994;120:835–54.
[4] Borodich FM. Fracture energy in a fractal crack propagating in concrete or rock. Doklady Rossiyskoy Akademii Nauk 1992;325:1138–41.
[5] Borodich FM. Fracture energy of brittle and quasi-brittle fractal cracks. In: Fractals in the natural and applied sciences, vol. A-41. North-Holland: Elsevier; 1994. p. 61–8.
[6] Borodich FM. Some fractal models of fracture. J Mech Phys Solids 1997;45:239–59.
[7] Borodich FM. Fractals and fractal scaling in fracture mechanics. Int J Fract 1999;95:239–59.
[8] Cherepanov GP, Balankin AS, Ivanova VS. Fractal fracture mechanics—a review. Engng Fract Mech 1995;51:997–1033.
[9] Mosolov AB. Cracks with fractal surfaces. Dokl Akad Nauk SSSR 1991;319:840–4.
[10] Mosolov AB. Fractal J-integral in fracture. Sov Tech Phys Lett 1991;17:698–700.
[11] Gol'dshteĭn RV, Mosolov AB. Cracks with a fractal surface. Sov Phys Dokl 1991;36:603–5.
[12] Gol'dshteĭn RV, Mosolov AB. Fractal cracks. J Appl Math Mech 1992;56:563–71.
[13] Yavari A, Hockett KG, Sarkani S. The fourth mode of fracture in fractal fracture mechanics. Int J Fract 2000;101:365–84.
[14] Yavari A, Sarkani S, Moyer ET. On fractal cracks in micropolar elastic solids. ASME J Appl Mech 2002;69(1):45–54.
[15] Yavari A, Sarkani S, Moyer ET. The mechanics of self-similar and self-affine fractal cracks. Int J Fract 2002;114(1):1–27.
[16] Yavari A. Generalization of Barenblatt's cohesive fracture theory for fractal cracks. Fractals 2002;10(2):189–98.
[17] Carpinteri A. Fractal nature of material microstructure and size effects on apparent mechanical properties. Mech Mater 1994;18:89–101.
[18] Carpinteri A. Scaling laws and renormalization groups for strength and toughness of disordered materials. Int J Solids Struct 1994;31:291–302.
[19] Carpinteri A, Chiaia B. Crack-resistance behaviour as a consequence of self-similar fracture topologies. Int J Fract 1996;76(4):327–40.
[20] Carpinteri A, Chiaia B. Power scaling laws and dimensional transitions in solid mechanics. Chaos, Solitions and Fractals 1996;7(9):1343–64.
[21] Carpinteri A, Chiaia B. Size effects on concrete fracture energy: dimensional transition from order to disorder. Mater Struct 1996;29:259–66.
[22] Harrison J, Norton A. Geometric integration on fractal curves in the plane. Indiana University Math J 1991;40:567–94.
[23] Harrison J. Numerical integration of vector fields over curves with zero area. Proc Am Math Soc 1994;121:715–23.
[24] Sih GC, Liebowitz H. Mathematical theories of brittle fracture. In: Liebowitz H, editor. Fracture, vol. II. New York: Academic Press; 1968. p. 67–190.
[25] Griffith AA. The phenomenon of rupture and flow in solids. Phil Trans Roy Soc London 1920;A221:163–98.

[26] Griffith AA. In: Proceedings of the 1st International Congress for Applied Mechanics, Delft, 1924. p. 55.
[27] Barenblatt GI. The mathematical theory of equilibrium cracks in brittle fracture. Adv Appl Mech 1962;7:55–129.
[28] Willis JR. A comparison of the fracture criteria of Griffith and Barenblatt. J Mech Phys Solids 1967;15:151–62.
[29] Rice JR. A path independent integral and the approximate analysis of strain concentration by notches and cracks. J Appl Mech 1968;35:379–86.
[30] Wnuk MP, co-author and editor, Nonlinear Fracture Mechanics. CISM Courses and Lectures No. 314, International Center for Mechanical Sciences, Springer Verlag, Udine, Italy; 1990.
[31] Wnuk MP, Legat J. Work of fracture and cohesive stress distributions resulting from triaxiality dependent cohesive model. Int J Fract 2001;114(1):29–46.
[32] Wnuk MP, Ramesham R, Bolin S. Advanced adhesion and bonding. JPL Publication D-17926, sponsored by NASA, publ. at Caltech-JPL; August 2000.
[33] Rice JR. Mathematical analysis in the mechanics of fracture. In: Liebowitz H, editor. Fracture, vol. II. New York: Academic Press; 1968. p. 191–311.